TEXTURE AUGMENTED ANALYSIS OF HIGH RESOLUTION SATELLITE IMAGERY IN DETECTING INVASIVE PLANT SPECIES

Fuan Tsai* and Ming-Jhong Chou

ABSTRACT

During recent decades, a considerable number of alien species have been brought into Taiwan and have caused significant impacts to local ecosystems and biodiversity. High resolution satellite imagery can provide detailed spatial characteristics over a large area and has a great potential for accurate vegetation mapping. However, most traditional multispectral image classification techniques focus on spectral discrimination of ground objects and may overlook useful spatial information provided by high resolution images. To achieve the best result, analysis of high resolution imagery should also incorporate spatial variations of the data. Therefore, this paper has looked into using a texture augmented procedure to analyze a high resolution satellite (QuickBird) image in order to detect an invasive plant species (*Leucaena leucocephala*) in southern Taiwan. Samples of primary vegetation covers were selected from the image to determine suitable texture analysis parameters for extracting texture features helpful for classification. Validation with ground truth data showed that the analysis produced high accuracies in detecting the target plant species and overall classification for primary vegetation types within the study site.

Key Words: remote sensing, texture analysis, GLCM, vegetation mapping.

I. INTRODUCTION AND BACKGROUND

The rapid spread of non-native plant species has caused significant impact to biodiversity and ecosystems world-wide. In Taiwan, surrounding oceans provide a natural barrier to prevent alien species from invading local ecosystems. However, during recent decades, a considerable number of alien species have been brought into the local environment due to increasing international travel and trading and for economic development purposes. A previous investigation (Lai, 1995) indicated that more than 4,500 known alien plant species had been brought into Taiwan legally or illegally by 1995. The spreading of alien species, especially those with aggressively invasive capability, is growing at an alarming rate. Among them, horse tamarind (*Leucaena leucocephala*) is one of the most serious invasive plant species and has colonized a great portion of the Kenting National Park and vicinity located on the Heng-Chun peninsula of southern Taiwan (Chiang & Hsu, 2000). In some of the areas within the national park, this tropical tree has completely replaced native tropical forests and shrubs and become the only dominant plant species (Liu & Chen, 2002).

Reducing the impact of alien species to local ecosystems and biodiversity and enforcing restoration and other remedy actions have become a trend in conservation (Stein & Flack, 1996). For researchers and decision makers to develop effective strategies to battle against this threatening situation and for resource management, it is necessary to obtain accurate species maps and to understand the severity of the invasions (Byers *et al*., 2002). Traditionally, this task relies heavily on field-based investigations that are usually expensive and time-consuming. Remote sensing, on the other hand, provides an opportunity for a timely and economical solution to discriminating invasive

*Corresponding author. (Email: ftsai@csrst.ncu.edu.tw)
The authors are with the Center for Space and Remote Sensing Research, National Central University, Zhong-Li, Taoyuan, Taiwan 320, R.O.C.

plant species from the local botanic community. For decades, aerial photographs and multispectral satellite images with low to moderate spatial resolutions, such as AVHRR, Landsat MSS, TM, SPOT and the like, were commonly used in a variety of remote sensing applications for vegetation mapping and have attained a certain success. For example, McCormick (1999) successfully produced a map of exotic vegetation using large-scale aerial photographs; Verheyden *et al.* (2002) also used aerial photos to monitor mangrove. A major disadvantage of using aerial photographs for vegetation mapping is that, even for an experienced operator, it still requires extensive interactive operations. The requirement of manual processing also creates another inconvenience, i.e. it may not be practical to use aerial photographs for an investigation over a large area.

Unlike aerial photographs, satellite imagery has large ground coverages and is provided in digital formats. Therefore, it is more suitable for automated image processing and analysis and is more practical for large areas of interest. Traditional multispectral satellite images have been successfully applied to vegetation-related studies from regional to local scales (Lins & Kleckner, 1996; Marino *et al.*, 1999; Townsend & Walsh, 2001; Wylie *et al.*, 2002). However, the broad spatial resolution and limited spectral information make it difficult, if not impossible, to achieve species-level classifications using traditional multispectral imagery.

As remote sensing instruments and technologies advance, new types of data have provided a great opportunity to identify specific plant species from remotely sensed images. One of the new remote sensing data is the so-called hyperspectral imagery that usually consists of tens to hundreds of spectral bands with fine spectral resolution. A few researchers have begun to explore hyperspectral remote sensing for detailed vegetation recognition and mapping wok. For example, Laba *et al*. (2005) successfully employed derivative spectral analysis (Tsai & Philpot, 1998; Tsai & Philpot, 2002) to analyze *in-situ* hyperspectral data for discriminating among alien plant species in wetlands; while Schmidt and Skidmore (2003) used a wavelet approach to separate vegetation types from field-collected spectra. Other algorithms to process and analyze hyperspectral images have also been proposed and have achieved successful results in vegetation mapping and species identification applications. For example, McGwire *et al*. (2000) developed a hyperspectral mixture model for quantitative analysis of sparse vegetation covers; Underwood *et al*. (2003) examined three spectral analysis methods for mapping nonnative plants from airborne hyperspectral images.

Another trend in remote sensing development is the improvement in spatial resolution. In contrast to the broad spatial resolution (usually more than 10 meters) of traditional multispectral satellite imagery, spaceborne images with ground resolution of several meters are ubiquitous and some (image systems) can even provide sub-meter level spatial details (e.g., IKONOS and QuickBird). Although still limited in spectral bands, high resolution satellite images can provide detailed spatial information like aerial photographs or other high resolution airborne data. Consequently, besides conventional spectral analysis, algorithms designed for investigating spatial patterns (textures) should also be used to process high resolution images for the best analysis and information retrieval.

Computerized texture analysis focuses on structural and statistical properties of spatial patterns appearing on digital images (Haralick *et al.*, 1973; Haralick, 1986). It has been successfully applied to forestry and vegetation studies with a variety of remote sensing data, including ground-based images (Tsheko, 2002), aerial photographs (Hudak & Wessman, 1998), multispectral images (Asner *et al*., 2002; Franklin *et al*., 2000; de Wasseige & Defourny, 2002) and radar images (Costa, 2004; Haack & Bechdol, 2000; Hess *et al*., 2003). Texture analysis of high resolution satellite images was also used for various vegetation-related applications, such as tree crown structure mapping (St-Onge & Cavayas, 1997), leaf-area-index (LAI) retrieval (Colombo *et al*., 2003), and most related to this study – plant species decomposition or extraction (Franklin *et al*., 2001; Katoh, 2004; Wang *et al*., 2004). In general, a previous study demonstrated that including texture into classification can increase the accuracy by 10% - 20% (Franklin *et al*., 2000).

Although texture analysis of remote sensing images has been proven to be a valid alternative and a valuable addition to vegetation-related applications, little has been done to design and establish guidelines and strategies for employing texture analysis in species-level applications, especially for the detection and monitoring of invasive plant species. Therefore, this study has investigated the use of texture analysis to enhance the analysis of high resolution imagery. The objective was to develop a systematic methodology that is effective and efficient in discriminating an invasive alien plant species (*Leucaena leucocephala*) from other vegetation cover in southern Taiwan using high resolution satellite images.

II. METHOD AND MATERIAL

1. Site and Target Descriptions

The site of this study is the Heng-Chun peninsula of southern Taiwan, including part of the Kenting National Park as well as private and public lands with moderate to high degrees of agricultural development (Fig. 1). The area has a rich population of vegetation.

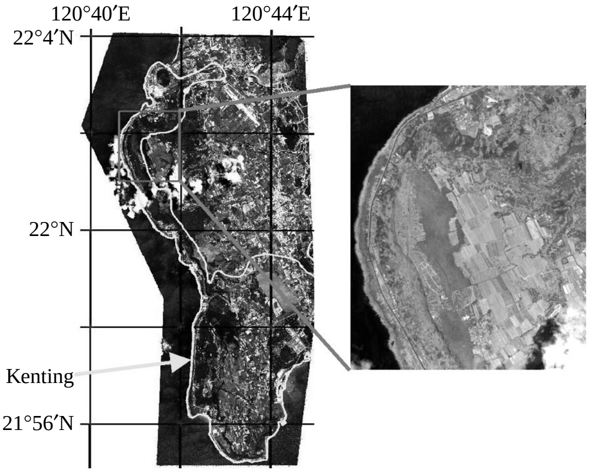

Fig. 1 Study site

Fig. 2 *Leucaena leucocephala* and its canopy structure (right)

The dominant species of wild plants in this area used to be Taiwan acacia (Acacia confusa). *Leucaena leucocephala* (Fig. 2) was imported in quantity from Latin America and planted in this area in the late 1970's for papermaking but was abandoned later in favor of other pulp sources. *Leucaena leucocephala* is a fast-growing deciduous tree. Because of its allelopathy and superior acclimation, it rapidly invaded local vegetation communities and gradually became a dominant species in Kenting National Park and vicinity (Chiang & Hsu, 2000; Liu & Chen, 2002). Other wild plants also exist, but they are sparse and difficult to observe on optical remote sensing images because they are usually blocked by acacia canopies. Consequently, three categories of vegetation land-cover types were used in the analysis of this research. They were: a) *Leucaena leucocephala* (the target); b) acacia; and c) farmland.

2. Material

The primary material to analyze in this study was a standard QuickBird multispectral and panchromatic high resolution satellite image set. The images were acquired in July, 2002. The nominal spatial resolutions of multispectral and panchromatic bands are 2m and 0.61m, respectively. After orthorectification, the image was first treated with a NDVI (Normalized Difference Vegetation Index) operation to identify regions covered by vegetation, using 0.6 as the threshold to distinguish vegetation and non-vegetation land-covers. A sub-image (4600 by 3800 pixels) of the study site was cropped out from the NDVI-treated image for subsequent analysis. The 0.6 NDVI threshold might seem to be conservatively high and could rule out sparse vegetation areas. Nonetheless, the dominant vegetation types, especially the target, of the study site tend to grow in close formation. Therefore, the exclusion of isolated, coarse vegetation covered pixels from the image should have little impact on the texture feature extraction for the identification of the target.

A vector layer of *Leucaena leucocephala* coverage produced after a 1996 survey conducted by a local research institute (Heng-Chun Research Center, Taiwan Forestry Research Institute) along with field-collected information and aerial photographs were used as supplementary data in this study to select training samples for classification and as part of the ground truth to verify results. The vector coverage was created by manual interpretation of aerial photographs from 1996. Experienced interpreters interactively examined orthorectified aerial-photos to identify boundaries of vegetation covered blocks and assess *Leucaena leucocephala* population densities of each block polygon. Because there were fluctuations of vegetation distributions in the study area between 1996 and 2002, the vector data were verified against more recent aerial photographs and field-investigated data to rule out incorrect polygons.

3. Texture Analysis and Procedure

The texture-augmented image analysis procedure is illustrated in Fig. 3. As mentioned before, after orthorectification and removal of non-vegetation areas, texture analysis was carried out on the high resolution (panchromatic) image of the study site to collect texture features that might be helpful in the detection of target species. The collected texture features were then sorted according to a principal component analysis (PCA). The first few principal component (PC) bands representing most of the variations were selected along with the original spectral band for a maximum likelihood classification and the classified result was verified against and evaluated by ground truth data.

Although there are variants of texture analysis methods, among them, gray level co-occurrence matrix (GLCM) algorithm (Haralick *et al*., 1973; Haralick, 1986) is probably the most commonly adopted for remote sensing. Previous studies indicated that GLCM is very suitable for finding texture information in images of natural scenes and performs well in classification

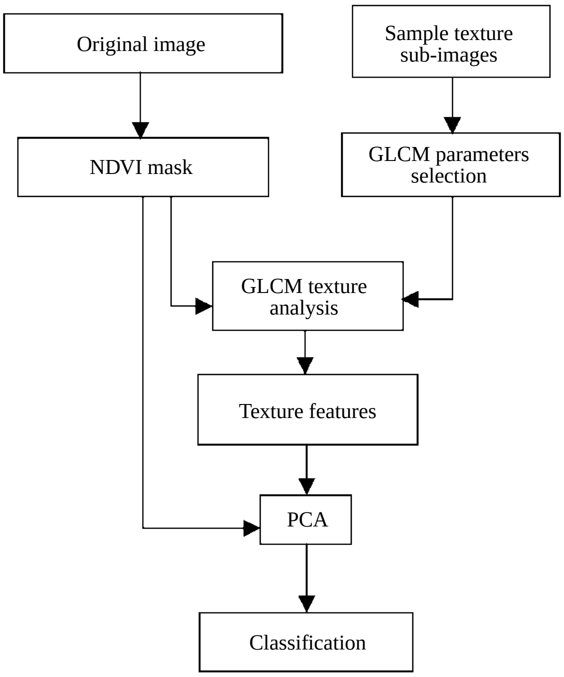

Fig. 3 Texture-augmented analysis procedure

applications (Hans du Buf *et al*., 1990; Ohanian & Dubes, 1992; Reed & Hans du Buf, 1993). Therefore, GLCM should also be an appropriate method of texture analysis in this project. GLCM quantifies texture by measuring the spatial frequency of co-occurrence of pixel gray levels in a user defined moving kernel (window) and forms a co-occurrence matrix of the kernel. After that, different statistical measures can be used to extract characteristics of the matrix that reflect spatial variations (textures features) of the window. For this paper, contrast, homogeneity, and entropy (Eqs. (1), (2) and (3)) were used for this purpose.

$$\text{Contrast: } \sum_{i,j=0}^{N-1} P_{i,j}(i-j)^2 \quad (1)$$

$$\text{Homogeneity: } \sum_{i,j=0}^{N-1} \frac{P_{i,j}}{1+(i-j)^2} \quad (2)$$

$$\text{Entropy: } -\sum_{i,j=0}^{N-1} (P_{i,j})\log(P_{i,j}) \quad (3)$$

where $P_{i,j}$ is the value of the (i, j) cell in a (normalized) co-occurrence matrix, and N is the gray level of the texture image.

As its name suggests, Contrast (also called sum of square variances) measures the weighted contrast of GLCM cells according to their distances to the matrix diagonal. The weighting of Contrast increases exponentially, so Contrast will result in a large number if there is great contrast in a window. On the other hand, homogeneity looks at the inverse difference moments and weights in a way inverse to Contrast. Therefore, it measures the "similarity" of the texture. The third statistical index, entropy, is related to the orderliness (uniformity) of the texture. Similar to physical entropy that refers to irremediable chaos, entropy of texture analysis evaluates how irregular or disorderly pixel values appear within a window. More detailed descriptions and discussions of the GLCM algorithm and these measures can be found in our listed references and image analysis texts and are not repeated in this paper.

Because the size of a GLCM matrix depends on the data range of pixel gray values, images of large numbers of data bits may result in large matrix sizes during GLCM operation and require a large amount of memory and CPU cycles to handle the computation. For example, the QuickBird image has 11-bit data, which yields a matrix size of more than four million cells (2048×2048) for a single pixel. As a result, it is a practical necessity to reduce the co-occurrence matrix size for better computational performance. More importantly, because GLCM approximates the joint probability distribution of two pixels, reducing the matrix size will also reduce the number of zero-value cells in a matrix, which in turn will improve the statistical validity. A common technique to reduce GLCM matrix sizes is to rescale image gray levels to a lower data bit number. Previous studies demonstrated that reduction of gray levels caused only minor degradation (about 3%) in classification accuracy (Marceau *et al*., 1990; Narayanan *et al*., 2000; Xu *et al*., 2003). Therefore, the original 11-bit QuickBird image used in this study was rescaled to 6-bit data before GLCM processing.

Another important factor that may cause substantial impacts to GLCM processing is the kernel size (Franklin *et al*., 1996; McGwire *et al*., 1993). To determine the most suitable kernel size for GLCM operation in this study, two sample sets of the three primary vegetation-cover types (Fig. 4) were selected from the panchromatic image of the study site for testing, using semivariance (Cohen *et al*., 1990; Hay *et al*., 1996) as the index. Semivariance is a measurement of data variations in the spatial domain. Let $Z(x_i)$ and $Z(x_i + h)$ be two pixel values with a lag of h (a vector of specific direction and distance). For all pixel pairs, $N(h)$, the semivariance $\gamma(h)$ is defined as:

$$\gamma(h) = \frac{1}{2N(h)} \sum_{i=1}^{N(h)} [Z(x_i) - Z(x_i + h)]^2 \quad (4)$$

A typical semivariance curve is as shown in Fig. 5. The purpose of the semivariance test is to determine the estimation of a lag (range) that will result in the maximum variability (sill) of a scene structure

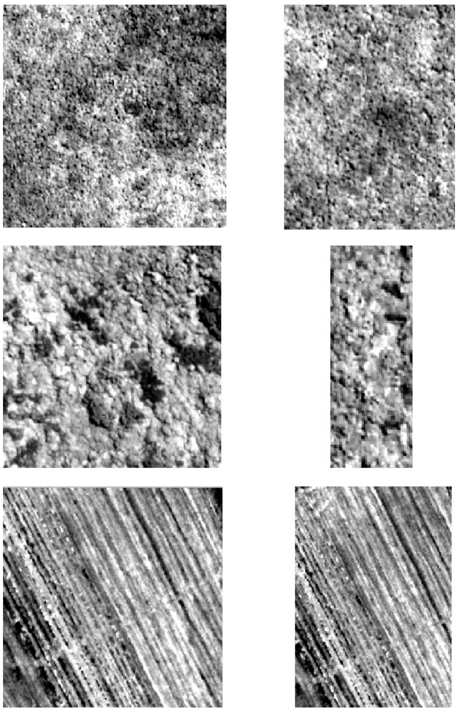

Fig. 4 Sample textures of *Leucaena leucocephala* (top), acacia (middle) and farmlands (bottom)

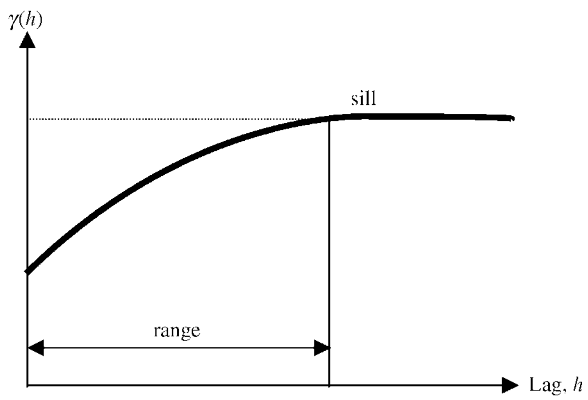

Fig. 5 Example semivarigram

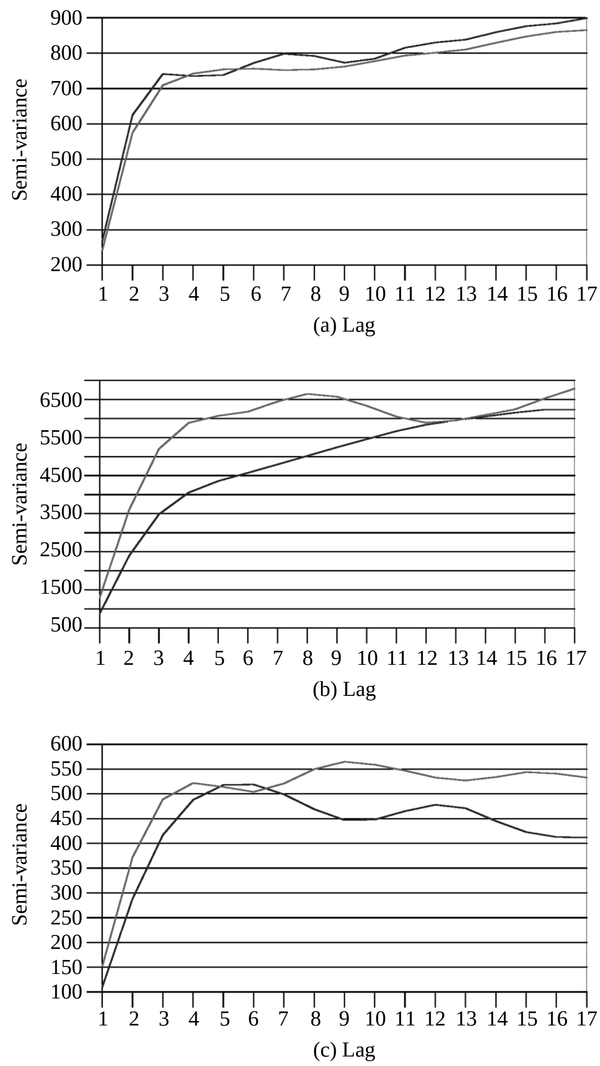

Fig. 6 Semivarigrams (a: *Leucaena*; b: acacia; c: farmland)

(Cohen *et al*., 1990; Hay *et al*., 1996) and use it as the GLCM kernel size. In this project, if the texture pattern of a specific plant is spatially independent, each vegetation type should have only one best estimated range in its semivarigrams. Results of semivariance tests on texture samples shown in Fig. 4 are displayed in Fig. 6, where each line represents the relationship between the semivariance and the lag of a sample texture image in Fig. 4. These results indicated that semivariances of *Leucaena* and acacia started to saturate at a lag of three while farmlands required five pixels of kernel size. (The best window size for acacia is arguable in Fig. 6, but the curves' curvatures shift at a lag of three.) Consequently, 3×3 and 5×5 were used as the moving window sizes of GLCM in this study. This should generate more effective texture characteristics of all three vegetation types than using a single kernel size; also it is more efficient than performing GLCM with an exhaustive series of kernel sizes.

Accordingly, GLCM matrices were calculated using 3×3 and 5×5 moving window sizes in four directions (0°, 45°, 90°, 135°) for contrast, homogeneity, and entropy measurements. This resulted in a total of 24 texture features. They were then passed down the processing pipeline for further feature reduction using PCA and selecting the first six PC bands that represent more than 95% of variations (Table I). Fig. 7 displays the selected PC texture features. As can be seen from the figure and Table 1, the fist PC band accounts for 78% of eigenvalues and likely represents most of the distinction among Leucaena and other plants.

Next, the collection of selected (texture) PC

Table 1 Eigen analysis of texture PC bands

	PC1	PC2	PC3	PC4	PC5	PC6
Eigenvalue	1839687.9	191561.1	63701.2	60291.1	41906.3	33083.7
%	78.8	8.2	2.73	2.58	1.79	1.42

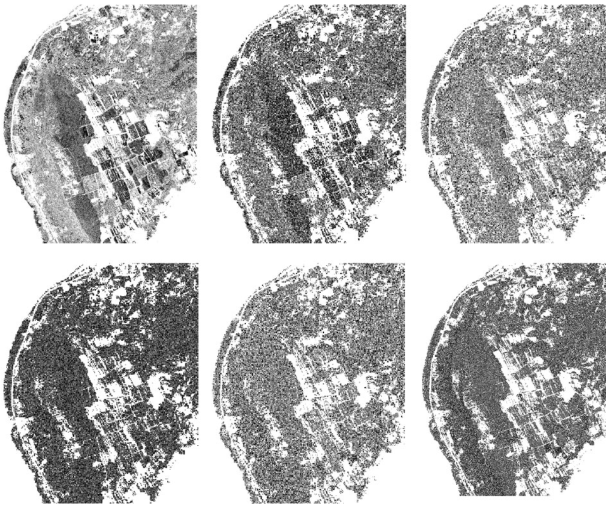

Fig. 7 Fist 6 PC textures (top: 1st, 2nd, 3rd; bottom: 4th, 5th, 6th)

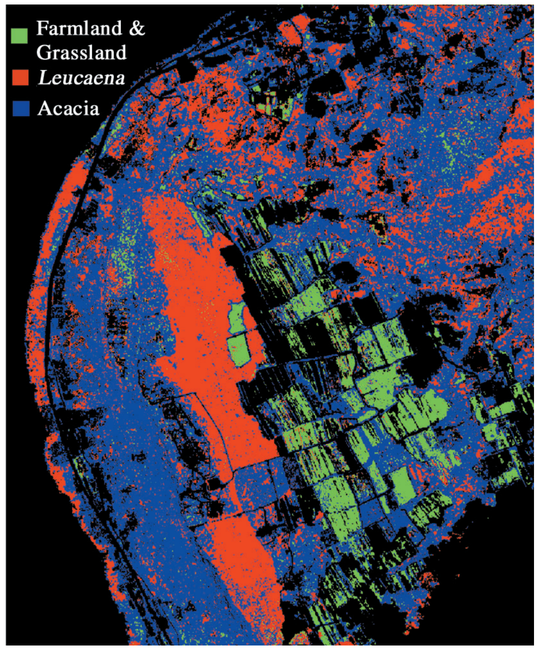

Fig. 8 Classification result

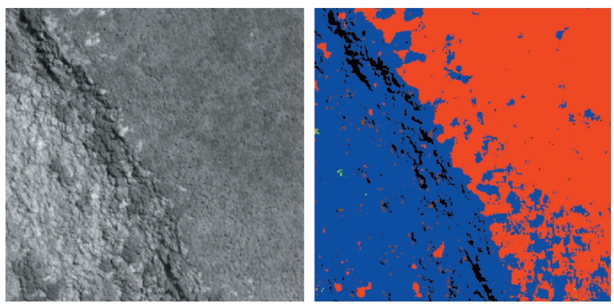

Fig. 9 Enlarged classification result of a region

features in conjunction with the original panchromatic spectral band were classified using a maximum likelihood classifier to categorize pixels into the three vegetation-cover types described in section II.1. The training data used in the classification were randomly selected pixels from areas identified from the 1996 vector layer, field survey maps and aerial photographs. Finally, the classification result was verified with ground truth data to assess the accuracy of *Leucaena leucocephala* mapping.

3. Results and Discussion

The classification result is displayed in Fig. 8. A quick visual inspection of the class image and comparison with aerial photographs shows that the texture-augmented classification has successfully discriminated the target (*Leucaena leucocephala*) from the other two vegetation-cover types. For example, Fig. 9 is the enlarged view of a region within the study site and the classification result. The lighter tone area with sphere-shaped canopy structures in the original image (left of Fig. 9) is acacia whereas the darker tone is the target. As can be seen from the classification (right of Fig. 9), the texture-augmented classification separated the two vegetation types effectively and correctly. A quick quantitative assessment shows that the overall accuracy is about 95.72% (61588/64746) for the area shown in Fig. 9.

To further analyze the performance of texture-augmented classification, additional quantitative and qualitative evaluations were conducted using two sets of ground truth data and from different perspectives. The first evaluation was done based on the 1996 vector layer of polygons mentioned in the previous section. Each polygon of the vector layer was assigned (by the original interpreter) an attribute indicating the level of *Leucaena leucocephala* population density (canopy coverage) within the polygon. The density of *Leucaena leucocephala* was marked as one of four levels: L1: 0%-25%; L2: 25%-50%; L3: 50%-75%; and L4: 75%-100%. These data were verified with more up-to-date

Table 2 L4 ground truth (75% - 100%) detection result

Polygon pixels	Identified pixels	Density	Polygon pixels	Identified pixels	Density
706	0	0	1168	587	0.5
6059	5600	0.92	176	176	1
4647	4503	0.97	16532	8368	0.5
3344	2926	0.88	3311	795	0.24
63497	58513	0.92	222	0 0	
1087	40	0.04	730	553	0.76
33	18	0.55	13958	8804	0.63
669	0	0	1616	426	0.26
1542	227	0.15	489	0	0
1263	34	0.03	291634	234468	0.8
1976	1	0	114662	109921	0.96
4002	472	0.12	38676	31294	0.81
1632	27	0.02	30348	18137	0.6
133	0	0	2887	191	0.07
2063	1720	0.83	232	39	0.17
656	528	0.8	8001	6811	0.85
1872	1587	0.85	880	866	0.98
2117	603	0.29	97594	83367	0.85
1416	1179	0.83	1339	159	0.12
4076	718	0.15	189	153	0.81

Accuracy = (635920/727434) = 87.42%

(year 2002) aerial photographs to remove polygons with outdated levels of density before they were adopted as the ground truth. For example, Fig. 10 displays an area in an aerial-photo, where the polygons were labeled as L4 in 1996 but the *Leucaena leucocephala* had been removed or replaced by other plants due to agricultural development or other reasons, so they were removed from the ground truth vector layer.

Using the corrected polygon layer as regions of interest (ROI's), a new population density of *Leucaena leucocephala* was calculated from the classification result for each ROI. Table 2 lists the new population densities after analysis of all L4 polygons for ground truth data. For each ROI, if the new density level matched the original one of that polygon, all pixels of the ROI were considered classified correctly. As a result, the classification accuracy of L4 regions (75%-100% of *Leucaena leucocephala*) is more than 87%.

From Table 2, it can be noted that most of the large polygons were classified correctly as L4 regions. The omissions primarily occurred for small polygons. It is possible that these areas were simply misclassified. Nonetheless, a careful verification with field maps revealed that most of these regions were located outside Kenting national park. Without the protection of the park, the vegetation coverage in these regions was more vulnerable to unnatural alternations and thus was removed or changed significantly because of land and other developments.

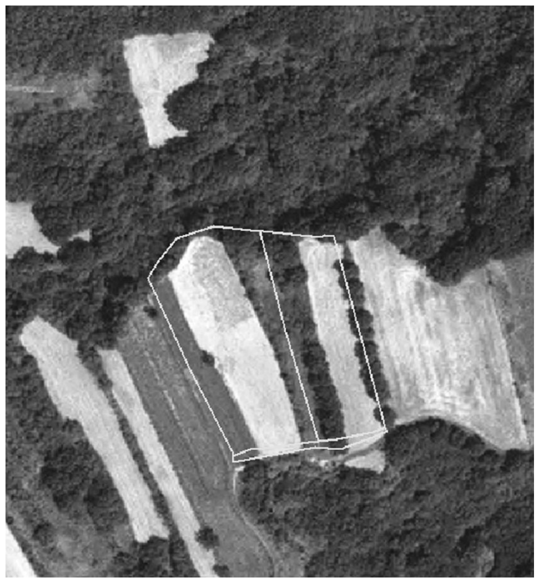

Fig. 10 Correction of vector layer with aerial photographs

The same procedure of (density level) accuracy assessment was performed for all other levels, and the result is listed in Table 3. As presented in the table, the overall classification accuracy is 84%. A thorough examination of Table 3 suggests that the

Table 3 Overall classification accuracy assessment

Level	# of polygons	Correctly identified	Total pixels	Identified pixels	Accuracy
L1 (0%—25%)	79	58	3586804	3133027	87.35%
L2 (25%—50%)	17	3	199322	33690	16.90%
L3 (50%—75%)	13	5	36963	22592	61.12%
L4 (75%—100%)	40	16	727434	635920	87.42%
Total			4550523	3825229	84.06%

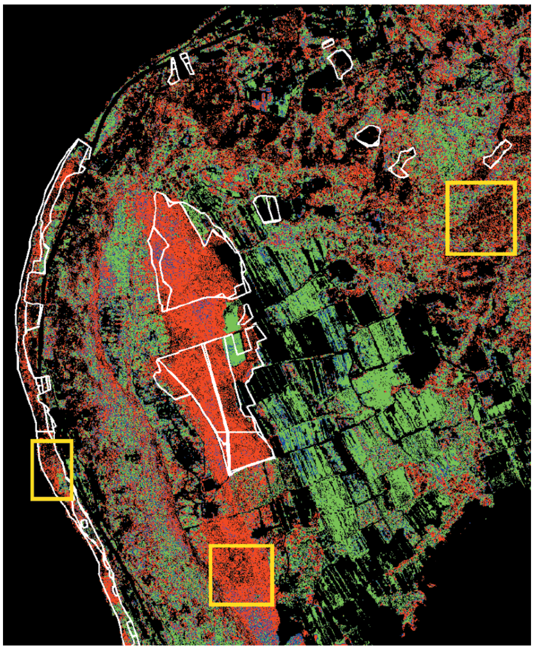

Fig. 11 Classification result using only the original panchromatic QuickBird image

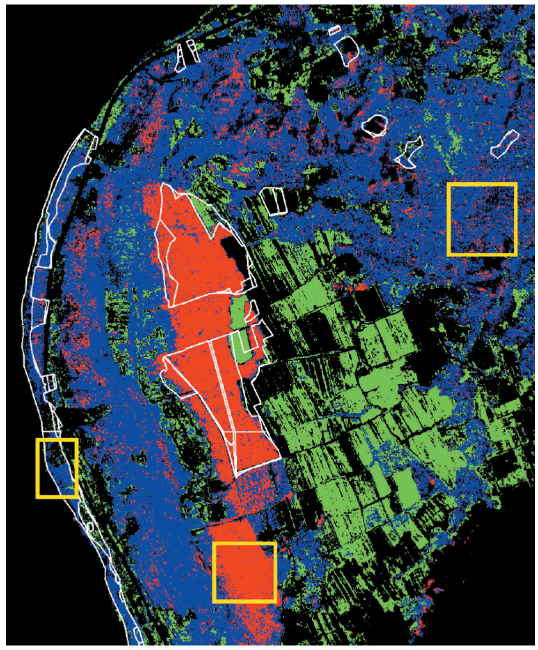

Fig. 12 Classification result using only the original multispectral QuickBird image

classifier worked very well in identifying regions with a high or low *Leucaena leucocephala* canopy coverage (L1 and L4 ROI's), although accuracies for moderate density levels (L2 and L3) are less accurate. This implies that the misclassification was largely confined to L2 and L3 and affected little of the L1 and L4 regions. The high omission in L2 and L3 classification does not necessarily imply that the classifier worked incorrectly for these regions. Most of the L2 and L3 polygons are small patches. The expected invasion of *Leucaena leucocephala* would substantially increase the density level of these regions. In addition, some of the polygons were close to agricultural zones outside the national park. Human activities could also alter their density levels.

For comparison and to further evaluate the performance of texture-augmented analysis, classification results of the original panchromatic and multi spectral images using the same training data but without adding any texture feature are displayed in Fig. 11 and Fig. 12, respectively. The overlaid (white) polygons on both figures are L4 regions of the ground truth. From Fig. 11, it is obvious that the classifier failed to identify most acacia pixels and the misclassification of *Leucaena leucocephala* is also evident. Comparing Fig. 8 and Fig. 12 with the original high resolution image shown in Fig. 1, it appears that a lot of *Leucaena leucocephala* (along the coastline, in particular) were misclassified as acacia in the multispectral image.

To evaluate the performance of target detection for the three data sets (panchromatic, multispectral, and texture-added), *Leucaena leucocephala* classification accuracies were calculated in three sub-areas marked by yellow rectangles in Figs. 11 and 12 (Area 1 to 3, from right to left) where *Leucaena leucocephala* is known to be the dominant plant species. The detection rates are listed in Table 4. In this table, the numbers of target pixels were counted from original high-resolution images and the "Detected" means the number of pixels correctly identified as the target. Therefore, Table 4 can be considered a validation of omission errors. On average, texture-added features

Table 4 *Leucaena leucocephala* detection rates in selected areas

	Panchromatic			Multispectral			Texture-added		
	Leucaena pixels	Detected	%	Leucaena pixels	Detected	%	Leucaena pixels	Detected	%
Area-1	125544	45448	36.2	11575	2489	21.5	125544	93617	74.57
Area-2	138111	108414	78.5	12562	12274	97.7	138111	120747	87.43
Area-3	24419	12311	50.42	2218	128	5.77	24419	19944	81.67
Average			57.68			56.5			81.34

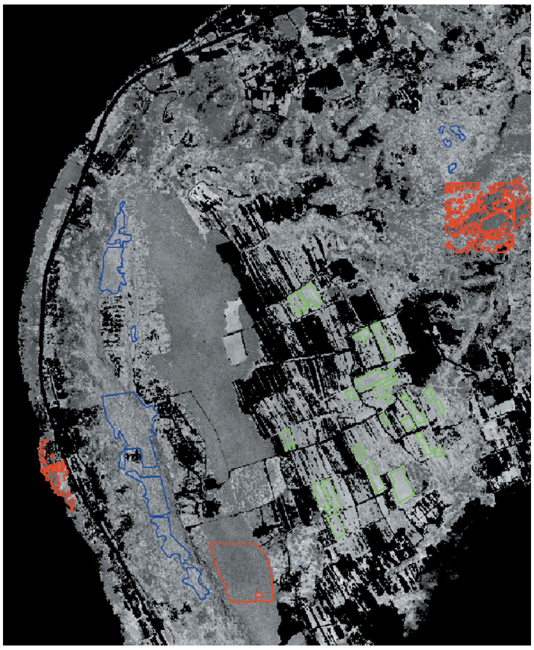

Fig. 13 Ground truth for verification (red: *Leucaena*; blue: acacia; green: farmlands)

generated the highest target detection rate. From Table 4, except in Area-2, where the target is almost "pure" (meaning they grow in more dense formation) within this area, texture-augmented outperformed the other two data sets significantly. Also, the extraordinarily low detection rate in Area-3 of multispectral data confirms the observation that multispectral images failed to provide distinct features for detecting the target in coastal zones.

Another evaluation and comparison of the classification for the three data sets but for all of the three primary vegetation types was made using selected ground truth data as displayed in Fig. 13 and the results are presented as confusion matrices in Table 5. From the data listed in Table 5, the Overall Accuracy (OA) and Kappa value of multispectral classification may seem to be slightly better than texture-augmented. However, careful examination of multispectral classification's error matrix (middle of Table 5) reveals that a large quantity of *Leucaena leucocephala* were misclassified as acacia in the multispectral data set. (This probably resulted from misclassification in coastal zones as described previously.) For the purpose of this study, the high omission error of the target (only 56% of Producer's Accuracy) in the multispectral image has made the classification result less reliable. On the other hand, the texture-augmented classification result exhibits equally good performance for both Producer's Accuracy and User's Accuracy, suggesting that the commission and omission errors are both inconsequential and the detection of the target is more successful. Therefore, for the purpose of detecting invasive plant species, the texture-augmented approach is considered more effective in *Leucaena leucocephal*a identification at the study site.

Comparing the result of texture-augmented classification to using only panchromatic data, it is clear that incorporating texture features into classification analysis has indisputably increased the effectiveness of detecting the target species and also improved the classification of other vegetation coverage. All in all, the examples and evaluations described in this section demonstrate that texture-augmented classification of high resolution imagery is an appropriate and convincing approach for detecting invasive plant species.

IV. CONCLUSIONS

This research employed a texture-augmented procedure to detect invasive plant species using high resolution satellite imagery. The analysis performed in this study demonstrates that integrating texture features into classification will enhance the performance of the classifier. The result of this study shows that texture-augmented classification of a high resolution satellite image can successfully detect an invasive plant species (*Leucaena leucocephala*) in Southern Taiwan. The procedure developed in this research can be used as a prototype for detecting and monitoring various invasive plant species with high resolution remote sensing imagery. However, there is still rooms for improvement. For example, although using semivariance to determine the best moving window size for calculating co-occurrence matrices

Table 5 Confusion matrices of classification results

Texture-added				
	Leucaena	Acacia	Farmlands	Producer's Acc.
Unclassified	7975	1048	1178	
Leucaena	257648	27879	1961	82.01%
Acacia	8484	235464	51681	82.07%
Farmlands	57	2525	139593	71.80%
Total	314164	286916	194413	
User's Acc.	89.62%	70.16%	86.08%	
OA = 80%; Kappa = 0.6877				

Multispectral				
	Leucaena	Acacia	Farmlands	Producer's Acc.
Unclassified	680	5	110	
Leucaena	15182	1274	0	56.37%
Acacia	11059	24608	176	93.91%
Farmlands	12	318	17381	98.38%
Total	6933	26205	7667	
User's Acc.	92.26%	68.65%	98.14%	
OA = 80.74%; Kappa = 0.7091				

Panchromatic				
	Leucaena	Acacia	Farmlands	Producer's Acc.
Unclassified	25132	18785	24939	
Leucaena	178289	81738	357	56.75%
Acacia	7647	64994	7133	22.65%
Farmlands	3096	121399	161984	3.32%
Total	314164	286916	194413	
User's Acc.	68.47%	81.47%	6.54%	
OA = 50.95%; Kappa = 0.3429				

from sample texture images is an effective approach, a more systematic algorithm should improve the efficiency of the process. A possible solution to this is to use a separability measurement, such as divergence or Jefferies-Matusita distance, to identify distinct texture features that are most helpful in separating target species from other objects. This can be done after the texture features are collected from the statistical measures of GLCM. The separability measurement can be used as a substitute for the PCA process of the developed procedure and thus eliminates the necessity of sophisticated eigen-system computation to increase the efficiency of the analysis.

From the result of this research, it is clear that *Leucaena leucocephala* has further invaded the local vegetation community and spread more widely in the study area during the past decade. The findings of this research have persuaded authorities to launch a full-scale investigation into the severity of *Leucaena leucocephala* invasion and the impact on local ecosystems in Kenting National Park and vicinity. Similar projects have also been initiated to review and map the invasions of other alien plant species in Taiwan. In addition, data collected in these projects will be valuable information to help prevent the situation from getting worse and for researchers and decision makers to work out countermeasures. This is an important step toward better preservation of biodiversity and protection of our fragile ecosystems.

ACKNOWLEDGMENTS

The authors would like to thank Dr. Hsiang-Hua Wang and the staff of Heng-Chun Research Center, Taiwan Forestry Research Institute for their assistance in the field work and ground truth collection. We also thank Prof. Pei-Fen Lee of National Taiwan University for providing aerial photographs and other valuable data. This research was supported in part by the Council of Agriculture and National Science Council (NSC 94-2752-M-008-004-PAE), Taiwan.

REFERENCES

Asner, G. P., Keller, M., Pereira, R., and Zweede, J. C., 2002, "Remote Sensing of Selective Logging in Amazon: Assessing Limitations Based on Detailed Field observations, Landsat ETM+, and Texture Analysis", *Remote Sensing of Environment*, Vol. 80, No. 3, pp. 483-496.

Byers, J. E., Richard, S. H., Randall, J. M., Parker, I. M., Smith, C. S., Lonsdale, W. M., Atkinson, I. A. E., Seastedt, T. R., Williamson, M., Chornesky, E., and Hayes, D., 2002, "Directing Research to Reduce the Impacts of Nonindigenous Species", *Conservation Biology*, Vol. 16, No. 3, pp. 630-640.

Chiang, M.-Y., and Hsu, L.-M., 2000, "The Wildization, Impacts, and Management of Non-native Plants in Taiwan" (in Chinese), *Proceedings of the Symposium on Bio-diversity and Preservation*, Taipei, Taiwan, pp. 399-411.

Cohen, W. B., Spies, T. A., and Bradshaw, G. A., 1990, "Semivariograms of Digital Imagery for Analysis of Conifer Canopy Structure," *Remote Sensing of Environment*, Vol. 34, No. 3, pp. 167-178.

Colombo, R., Bellingeri, D., Fasolini, D., and Marino, C. M., 2003, "Retrieval of Leaf Area Index in Different Vegetation Types Using High Resolution Satellite Data", *Remote Sensing of Environment*, Vol. 86, No. 1, pp. 120-131.

Costa, M. P. F., 2004, "Use of SAR Satellite for Mapping Zonation of Vegetation Communities in the Amazon Floodplain", *International Journal of Remote Sensing*, Vol. 25, No. 10, pp. 1817-1835.

Franklin, S. E., Wulder, M. A., and Lavigne, M. B., 1996, "Automated Derivation of Geographic Window Size for Remote Sensing Digital Image Texture Analysis", *Computers & Geosciences*, Vol. 22, No. 6, pp. 665-673.

Franklin, S. E., Hall, R. J., Moskal, L. M., Maudie, A. J., and Lavigne, M. B., 2000, "Incorporating Texture into Classification of Forest Species Composition from Airborne Multispectral Images", *International Journal of Remote Sensing*, Vol. 21, No. 1, pp. 61-79.

Franklin, S. E., Wulder, M. A., and Gerylo, G. R., 2001, "Texture Analysis of IKONOS Panchromatic Data for Douglas-fir Forest Age Class Separability in British Columbia", *International Journal of Remote Sensing*, Vol. 22, No. 13, pp. 2627-2632.

Haack, B., and Bechdol, M., 2000, "Integration Multisensor Data and RADAR Texture Measurement for Landcover Mapping", *Computers & Geosciences*, Vol. 26, No. 4, pp. 411-421.

Hans du Buf, J. M., Kardan, M., and Spann, M., 1990, "Texture Feature Performance for Image Segmentation", *Pattern Recognition*, Vol. 23, No. 3, pp. 291-309.

Haralick, R. M., Shanmugam, K., and Dinstein, I., 1973, "Texture Features for Image Classification", *IEEE Transactions on Systems, Man, and Cybernetics*, Vol. 3, pp. 610-621.

Haralick, R. M., 1986, "Statistical Image Texture Analysis", *Handbook of Pattern Recognition and Image Processing*, Young, T.Y. & Fu, K.S., ed., Academic Press, New York, USA, pp. 247-279.

Hay, G. L, Niemann, K. O., and McLean, G., 1996, "An Object-specific Image-texture Analysis of H-resolution Forest Imagery", *Remote Sensing of Environment*, Vol. 55, No. 2, pp. 108-122.

Hess, L. L., Melack, J. M., Novo, E. M., Barbosa, C. C. F., and Gastil, M., 2003, "Dual-Season Mapping of Wetland Inundation and Vegetation for the Central Amazon Region", *Remote Sensing of Environment*, Vol. 87, No. 4, pp. 404-428.

Hudak, A. T., and Wessman, C. A., 1998, "Texture Analysis of Historical Aerial Photography to Characterize Woody Plant Encroachment in South African Savanna - II. Real Digital Images", *Remote Sensing of Environment*, Vol. 66, No. 3, pp. 317-330.

Katoh, M., 2004, "Classifying Tree Species in a Northern Mixed Forest Using High-resolution IKONOS Data", *Journal of Forest Research*, Vol. 9, No. 1, pp. 7-14.

Laba, M., Tsai, F., Ogurcak, D., Smith, S., and Richmond, M. E., 2005, "Use of Derivative Analysis for the Spectral Discrimination of Invasive Wetland Plant Species", *Photogrammetric Engineering and Remote Sensing*, Vol. 71, No. 5, pp. 603-611.

Lai, M. J., 1995, *Directories of Botanic Species in Taiwan* (in Chinese), Di-Jing Press, Taipei, Taiwan.

Lins, K. F., and Kleckner, R., 1996, "Land Use and Land Cover Mapping in the United Sates: An Overview and History of the Concept", *GAP Analysis: A Landscape Approach to Biodiversity Planning*, J. M. Scott et al., ed., ASPRS, Bethesda, MD, USA, pp. 57-65.

Liu, F.-Y., and Chen, M.-A., 2002, "The Impacts of Alien Plants to Native Vegetation Ecosystems in Kenting National Park - An Example of Leucaena leucocephala" (in Chinese), *Conservation Research Report No. 112*, Kenting National Park, Taiwan.

Marceau, D. J., Howarth, P. J., Dubois, J. M., and Gratton, D. J., 1990, "Evaluation of the Grey-level Co-occurrence Matrix Method for Land-Cover Classification Using SPOT Imagery", *IEEE Transactions on Geoscience & Remote Sensing*, Vol. 28, No. 4 , pp. 513-519.

Marino, B. D. V., Geiss, P., O'Connell, B., Dieter, N., Burgess, T., Roberts, C., and Lunine, J., 1999, "Multispectral Imaging of Vegetation at Biosphere 2", *Ecological Engineering*, Vol. 13, No. 1, pp. 321-331.

McCormick, C. M., 1999, “Mapping Exotic Vegetation in the Everglades Using Large-scale Serial Photographs”, *Photogrammetric Engineering and Remote Sensing*, Vol. 65, No. 2, pp. 179-184.

McGwire, K., Friedl, K. M., and Estes, J. E., 1993, “Spatial Structure, Sampling Design and Scale in Remotely-sensed Imagery of a California Savanna Woodland”, *International Journal of Remote Sensing*, Vol. 14, No. 11, pp. 2137-2164.

McGwire, K., Minor, T., and Fenstermaker, L., 2000, “Hyperspectral Mixture Modeling for Quantifying Sparse Vegetation Cover in Arid Environments”, *Remote Sensing of Environment*, Vol. 72, No. 3, pp. 360-374.

Narayanan, R. M., Sankaravadivelu, T. S., and Reichenbach S. E., 2000, “Dependence of Image Information Content on Gray-scale Resolution”, *Proceedings of IGARSS 2000*, Vol.1, pp. 153-155.

Ohanian, P. P., and Dubes, R. C., 1992, “Performance Evaluation of Four Classes of Textural Features”, *Pattern Recognition*, Vol. 25, No. 8, pp. 819-833.

Podest, E., and Saatchi, S., 2002, “Application of Multiscale Texture in Classifying JERS-1 Radar Data over Tropical Vegetation”, *International Journal of Remote Sensing*, Vol. 23, No. 7, pp. 1487-1506.

Reed, T. R., Hand du and Buf, J. M., 1993, “A Review of Recent Texture Segmentation and Feature Extraction Techniques”, *CVGIP: Image Understanding*, Vol. 57, No. 3, pp. 359-372.

Schmidt, K. S., and Skidmore, A. K., 2003, “Spectral Discrimination of Vegetation Types in Coastal Wetland”, *Remote Sensing of Environment*, Vol. 85, No. 1, pp. 92-108.

Stein, B. A., and Flack, S. R., 1996, *American’s Least Wanted: Alien Species Invasions of US Ecosystems*, The Nature Conservancy, Arlington, VA, USA.

St-Onge, B. A., and Cavayas, F., 1997, “Automated Forest Structure Mapping from High Resolution Imagery Based on Directional Semivariogram Estimates”, *Remote Sensing of Environment*, Vol. 61, No. 1, pp. 82-95.

Townsend, P. A., and Walsh, S. J., 2001, “Remote Sensing of Forested Wetland: Application of Multitemporal and Multispectral Satellite Imagery to Determine Plant Community Composition and Structure in Southeastern USA”, *Vegetatio*, Vol. 157, No. 2, pp. 129-149.

Tsai, F., and Philpot, W. D., 1998, “Derivative Analysis of Hyperspectral Data”, *Remote Sensing of Environment*, Vol. 66, No. 1, pp. 41-51.

Tsai, F., and Philpot, W., 2002, “A Derivative-Aided Image Analysis System for Land-cover Classification”, *IEEE Transactions on Geoscience & Remote Sensing*, Vol. 40, No. 2, pp. 416-425.

Tsheko, R., 2002, “Discrimination of Plant Species Using Co Occurrence Matrix of Leaves”, *Agricultural Engineering International: the CIGR Journal of Scientific Research & Development*, Vol. 4, May 2002, e-journal: http://cigr-ejournal.tamu.edu/volume4.html/

Underwood, E., Ustin, S., and DiPietro, D., 2003, “Mapping Nonnative Plants Using Hyperspectral Imagery”, *Remote Sensing of Environment*, Vol. 86, No. 2, pp. 150-161.

Verheyden, A., Dahdouh-Guebas, F., Thomas, K., DeGenst W., Hettiarachchi, S., and Koedam, N., 2002, “High-Resolution Vegetation Data for Mangrove Research As Obtained From Aerial Photographs”, *Environment, Development and Sustainability*, Vol. 4, No. 2, pp. 113-133.

Wang, L., Sousa, W. P., Gong, P., and Biging, G. S., 2004, “Comparison of IKONOS and QuickBird Images for Mapping Mangrove Species on the Caribbean Coast of Panama”, *Remote Sensing of Environment*, Vol. 91, No. 4, pp. 432-440.

de Wasseige, C., and Defourny, P., 2002, “Retrieval of Tropical Forest Structure Characteristics from Bi-directional Reflectance of SPOT Images”, *Remote Sensing of Environment*, Vol. 83, No. 3, pp. 362-375.

Wylie, B. K., Meyer, D. J., Tieszen L. L., and Mannel S., 2002, “Satellite Mapping of Surface Biophysical Parameters at the Biome Scale over the North American Grassland – A Case Study”, *Remote Sensing of Environment*, Vol. 79, No. 2, pp. 266-278.

Xu, B., Gong, P., Seto, E., and Spear, R., 2003, “Comparison of Gray Level Reduction Schemes with A Revised Texture Spectrum Method for Land-use Classification Using IKONOS Imagery”, *Photogrammetric Engineering and Remote Sensing*, Vol. 69, No. 5, pp. 529-536.

Manuscript Received: Feb. 15, 2005
Revision Received: Aug. 09, 2005
and Accepted: Aug. 22, 2005